



American Society of Hematology
2021 L Street NW, Suite 900,
Washington, DC 20036
Phone: 202-776-0544 | Fax 202-776-0545
editorial@hematology.org

Single cell analysis reveals immune dysfunction from the earliest stages of CLL that can be reversed by ibrutinib

Tracking no: BLD-2021-013926R2

Noelia Purroy Zuriguel (Dana-Farber Cancer Institute; Harvard Medical School, United States) Yuzhou Tong (Dana-Farber Cancer Institute; Harvard Medical School, United States) Camilla Lemvig (Technical University of Denmark, Denmark) Nicoletta Cieri (Dana-Farber Cancer Institute, United States) Shuqiang Li (Broad Institute, United States) Erin Parry (Dana-Farber Cancer Institute, United States) Wandu Zhang (Dana-Farber Cancer Institute, United States) Laura Rassenti (University of California, San Diego, United States) Thomas Kipps (Moore's Cancer Center, University of California, United States) Susan Slager (Mayo Clinic, United States) Neil Kay (Mayo Clinic, United States) Connie Lesnick (Mayo Clinic,) Tait Shanafelt (Stanford University School of Medicine, United States) Paolo Ghia (Università Vita-Salute San Raffaele, Italy) Lydia Scarfò (Laboratory of B cell Neoplasia, Division of Experimental Oncology, Istituto Scientifico San Raffaele, Italy) Kenneth Livak (Dana-Farber Cancer Institute, United States) Peter Kharchenko (Harvard Medical School, United States) Donna Neuberg (Dana-Farber Cancer Institute, United States) Lars Ronn Olsen (Technical University of Denmark, Denmark) Jean Fan (Johns Hopkins University, United States) Satyen Gohil (University College London, United Kingdom) Catherine Wu (Dana-Farber Cancer Institute; Harvard Medical School, United States)

Abstract:

Conflict of interest: COI declared - see note

COI notes: N.P. is currently an employee of AstraZeneca; CJW holds equity in BioNTech, Inc.; and receives research funding from Pharmacyclics; SHG has received speaker fees from Janssen UK, travel and honoraria from Abbvie, and undertakes research consultancy for Novalgen Limited. P.G. received honoraria from AbbVie, AstraZeneca, ArQule (MSD, BeiGene, Celgene/Juno/BMS, Janssen, Loxo/Lilly, Roche and research funding from AbbVie, AstraZeneca, Janssen, Sunesis. P.V.K serves on the Scientific Advisory Board to Celsius Therapeutics Inc. and Biomage Inc. N.E.K. Advisory Board for: Abbvie, Astra Zeneca, Behring, Cytomx Therapy, Dava Oncology, Janssen, Juno Therapeutics, Oncotracker, Pharmacyclics and Targeted Oncology. DSMC (Data Safety Monitoring Committee) for: Agios Pharm, AstraZeneca, BMS -Celgene, Cytomx Therapeutics, Janssen, Morpho-sys, Rigol. Research funding from: Abbvie, Acerta Pharma, Bristol Meyer Squib, Celgene, Genentech, MEI Pharma, Pharmacyclics, Sunesis, TG Therapeutics, Tolero Pharmaceuticals. L.S. received honoraria from AbbVie, AstraZeneca, Janssen and travel funding from Janssen. T.D.S. received research support to institution from Genentech, Pharmacyclics.

Preprint server: No;

Author contributions and disclosures: N.P., J.F., S.H.G. and C.J.W. designed and conceived the study; N.P., L.Z.R., T.J.K., S.L.S., N.E.K., C.L., T.D.S., P.G., and L.S. collected samples and clinical annotations; S.L. generated the single cell RNAseq libraries and processed the raw sequencing data; N.P., Y.E.T., C.K.L., N.C., E.M.P., D.S.N., J.F., and S.G. analyzed and interpreted data; J.F., S.G. and C.J.W. supervised the project; N.P., Y.T., S.G., and C.J.W. wrote the paper with assistance from all other authors.

Non-author contributions and disclosures: No;

Agreement to Share Publication-Related Data and Data Sharing Statement: We will deposit all single cell data into a public repository (dbGAP). Questions from readers regarding methods and protocols will be answered by email to the corresponding author. The dbGAP number for this study is Phs002705.v1.

Clinical trial registration information (if any):

1 **Title**

2 Single cell analysis reveals immune dysfunction from the earliest stages of CLL that can be
3 reversed by ibrutinib

4

5 **Authors**

6 Noelia Purroy^{1,2,3*}, Yuzhou Evelyn Tong^{2,3,14*}, Camilla K. Lemvigh^{1,4*}, Nicoletta Cieri^{1,2,3},
7 Shuqiang Li^{3,5}, Erin M. Parry^{1,2,3}, Wandi Zhang¹, Laura Z. Rassenti⁶, Thomas J. Kipps⁶, Susan L.
8 Slager⁷, Neil E. Kay⁸, Connie Lesnick⁸, Tait D. Shanafelt⁹, Paolo Ghia¹⁰, Lydia Scarfò¹⁰,
9 Kenneth J Livak^{1,5}, Peter V. Kharchenko¹¹, Donna S Neuberg¹², Lars Rønn Olsen⁴, Jean Fan¹⁶,
10 Satyen H. Gohil^{1,2,3,15} and Catherine J. Wu, MD^{1,2,3,13,†}

11

12 **Affiliations**

13 ¹Department of Medical Oncology, Dana Farber Cancer Institute, Boston, MA; ²Harvard
14 Medical School, Boston, MA, USA; ³Broad Institute, Cambridge, MA, USA; ⁴Department of
15 Health Technology, Technical University of Denmark, Kongens Lyngby, Denmark;
16 ⁵Translational Immunogenomics Lab, Dana Farber Cancer Institute, Boston, MA, USA; ⁶Moore's
17 Cancer Center, University of California, San Diego, La Jolla, CA, USA; ⁷Department of Health
18 Sciences Research, Mayo Clinic, Rochester, MN, USA; ⁸Department of Medicine, Mayo Clinic,
19 Rochester, MN, USA; ⁹Stanford University, Stanford, CA, USA; ¹⁰Division of Experimental
20 Oncology and Department of Onco-Hematology, Università Vita-Salute San Raffaele and
21 Istituto di Ricovero e Cura a Carattere Scientifico (IRCCS) Ospedale San Raffaele, Milano,
22 Italy; ¹¹Department of Biomedical Informatics, Harvard Medical School, Boston, MA, USA;
23 ¹²Department of Data Science, Dana-Farber Cancer Institute, Boston, MA, USA; ¹³Division of

24 Hematology, Department of Medicine, Brigham and Women's Hospital, Boston, MA, USA.

25 ¹⁴Program in Health Sciences & Technology, Harvard Medical School & Massachusetts Institute

26 of Technology, Boston, MA, USA; ¹⁵Department of Academic Haematology, University College

27 London, UK; ¹⁶Department of Biomedical Engineering, Johns Hopkins University, Baltimore,

28 MD, USA.

29 * denotes equal contribution

30 † corresponding author

31

32 **Correspondence to:** cwu@partners.org

33

34 **Word count:** 1385

35 Chronic lymphocytic leukemia (CLL) is characterized by a clonal expansion of mature

36 CD19⁺CD5⁺ B cells, which are highly dependent on microenvironmental cues for their survival¹.

37 This common adult leukemia is preceded by a precursor phase termed monoclonal B-cell

38 lymphocytosis (MBL)^{2,3} that has been characterized as indistinguishable from CLL at the

39 genetic, transcriptomic and epigenomic level⁴⁻⁶. However, how leukemia cells co-evolve with

40 immune cells in their circulating microenvironment during the onset of MBL and upon

41 progression to CLL remains incompletely characterized⁷.

42

43 Recently, single cell transcriptome sequencing approaches (scRNA-seq) have transformed our

44 ability to gain a comprehensive evaluation of the spectrum of immune cells within the tumor

45 microenvironment and of their potential crosstalk with cancer cells⁸⁻¹⁴. Herein, we applied

46 scRNA-seq to broadly characterize circulating immune cells co-existing with leukemic cells

47 during natural CLL progression. Although we acknowledge the critical role of bone marrow and
48 lymph nodes microenvironment on CLL cells, the lack of feasibility for procuring serial
49 specimens from these tissue compartments led us to focus our study on circulating immune cells.
50 We therefore collected serial peripheral blood mononuclear cell (PBMC) samples from 3
51 individuals with high count MBL who did not progress to CLL after a median follow-up of 7.0
52 years and 7 patients with CLL, whose genetic characterization of CD19⁺CD5⁺ cells over time by
53 whole-exome sequencing (WES), has been previously reported¹⁵ (**Figure 1A**). For all patients,
54 we processed paired samples: the first time point (T1) was collected at a median of 4.96 years
55 (range: 2.44-5.46) from MBL diagnosis or 2.54 years (range: 0.5-4.2) from CLL diagnosis; while
56 the second time point (T2) was collected at a median of 2.97 years (range: 2.01-2.99) from T1
57 for the MBL patients and 4.75 years (range: 1.3-10.6) for the CLL patients. T2 samples for CLL
58 patients were collected at a median of 0.2 years (range: 0-5.9) before first treatment (**Suppl**
59 **Table 1**).

60
61 Non-CD19⁺CD5⁺ cells were isolated by fluorescence-activated cell sorting and samples from
62 each patient were processed on the same day to minimize batch effect. Cell suspensions were
63 loaded on a GemCode Single-Cell Instrument (10x Genomics) and libraries were prepared as
64 previously described¹⁶ (**Suppl Methods**). Analysis was conducted using Seurat V4.0.0 selecting
65 cells with gene count between 500 and 3,000 and less than 10% mitochondrial reads. Using the
66 trimmed dataset, we isolated the non-tumor population and assigned immune cell types by
67 performing multimodal reference mapping using a CITE-seq reference of 162,000 PBMCs
68 measured with 228 antibodies¹⁷. B cells were excluded due to potential CLL contamination.
69 After quality control, we obtained 67,333 single cell transcriptomes (median number of cells per

70 sample: 3711, range 491-6633 cells) (**Figure 1B, Suppl Table 1**). For each sample, we evaluated
71 the potential for processing and batch artefacts between samples and cohorts, and we selected
72 cohorts with similar ‘cold-shock signature’¹⁸ for comparison (**Suppl Figure 1A**). In total, we
73 identified 16 clusters across 3 distinct lineages: T cells, NK cells and myeloid cells (**Figure 1B,**
74 **top UMAP**). The distribution of immune cell types from MBL and CLL samples and across
75 patients appeared to be balanced across the cell clusters (**Figure 1B, bottom UMAP; Suppl**
76 **Figure 1B**). Analysis of the proportions of immune cell types, including various T cell subsets,
77 between MBL and CLL samples revealed no differences, even across time points (T1 vs T2)
78 (**Figure 1C-D; Suppl Table 2a**).

79
80 To confirm the absence of major differences in immune cell proportions between MBL and CLL,
81 we performed scRNAseq on PBMCs collected from a separate cohort of 4 high count MBL
82 patients that progressed to CLL (MBL-CLL1-4); the median time from MBL (T1) to CLL
83 diagnosis was 2.68 years (range, 0.7 – 4.6) and from CLL diagnosis to T2 was 0.6 years (range, 0
84 – 1.8). We also evaluated 2 age-matched healthy donors (HDs, median number of cells per
85 sample: 4400, range 2630-7596 cells) using the same approach described above (**Figure 2A, B**).
86 Again, we observed an absence of major compositional or phenotypic changes in immune cell
87 populations in the transition from MBL to CLL, while marked differences in the composition in
88 immune cell types were evident in CLL compared to HDs. In particular, the proportion of CD8⁺
89 T cells was higher in CLL compared to HD (33% vs 8%, p=0.037), with a corresponding
90 decrease in CD4⁺ T cells (**Figure 2C, left panel; Suppl Table 2b**). The CD4⁺ and CD8⁺ T cell
91 subtypes that contributed to these differences were naïve, central memory (TCM) CD4⁺ and
92 terminal effector memory (TEM) CD8⁺ cells (**Figure 2C, right panel**). A higher number of

93 differentially expressed genes (DESeq adjusted p-value <0.05 and $|\text{avg_log}_2\text{FC}| >0.6$) was
94 observed between HD and MBL/CLL patients than between MBL to CLL at the time of
95 progression (MBL-CLL 1 and 2, **Figure 2D**; **Suppl Table 3**). More differences in gene
96 expression were seen in those paired samples where CLL was sampled at a time more distant
97 from transition to CLL (MBL-CLL 3 and 4), suggesting further evolution of the immune
98 response over time with CLL progression. Effector memory CD8^+ T cells, CD56^{dim} NK cells
99 consistently showed more differentially expressed genes in both MBL and CLL versus HDs
100 (**Figure 2D right panel**), which we also observed when re-analyzing these data as a pseudo-bulk
101 analysis of the same data (**Suppl Fig 2**). Comparable shifts in immune cell expression profiles
102 were observed in the evaluation of independent MBL (MBL1-3, T1) versus CLL (CLL1-7, T2),
103 but only minimal differences were observed in non-progressing MBL (**Figure 2E**). While we
104 acknowledge that the low number of replicates ($n=2$) does not provide sufficient power to detect
105 the biological variability among HDs and that individual-specific variations might confound the
106 observed differences between HDs and MBL/CLL samples, we minimized this risk by selecting
107 age-matched HDs and applied uniform processing to all samples.

108

109 To investigate which dysfunctional immune mechanisms may potentially impact CLL biology,
110 we interrogated major molecular interactions between immune and normal B or CLL-B cells in
111 HDs or patients, respectively, using CellPhoneDB v2.1.7 which predicts potential interactions
112 between ligand–receptor pairs based on elevated expression in the corresponding cell-types¹⁹. In
113 so doing, we observed an increased total number of potential interactions in subjects with MBL
114 compared to HDs. This increase remained stable with progression to CLL and was evident across
115 diverse immune cell types but most distinctly observed in monocytes (**Figure 2F, left heatmap**).

116 To examine the effects of B cell receptor (BCR) signaling inhibition with ibrutinib on the
117 cellular interactions between immune and leukemia cells, we re-analyzed 4 additional scRNA-
118 seq samples previously generated from PBMCs before and during ibrutinib treatment (cells
119 collected 30-240 days after treatment) from two patients with CLL^{20,21}. We again observed that
120 the number of cellular interactions in pre-treatment CLL samples was higher across immune cell
121 types and especially in monocytes in both patients. Consistently, the number of interactions
122 decreased after ibrutinib treatment to levels similarly observed in HDs (**Figure 2F, right**
123 **heatmaps**). Most of the interactions upregulated in MBL/CLL patients involved inhibitory
124 signals of immune cell function proceeding from CLL cells across to various immune cell types
125 such as: *BTLA/MIF-TNFRSF14* (*HVEM*, observed in MBL-CLL1, 3 and 4), *CTLA4-CD86*
126 (observed in MBL-CLL4), and *LGALS9-HAVCR2* (*TIM3*, observed in MBL-CLL1-4) (**Figure**
127 **2G, left panel and Suppl Fig 3**). Notably, only a proportion of cancer cells express these
128 inhibitory signals: *BTLA* (17.4%), *MIF* (41.6%), *LGALS9* (18.2%), and *CTLA4* (10.4%) (**Suppl**
129 **Fig 4**). We observed that all these interactions were downregulated after ibrutinib treatment
130 (**Figure 2G, right panels**).

131

132 Altogether, we observed that the composition and state of immune cells was markedly different
133 between HDs and MBL patients, while no major additional transcriptional changes manifested
134 during natural progression from MBL to CLL. These observations suggest that the key drivers of
135 transcriptional immune dysfunction in CLL may be present early during the course of the disease
136 and are in keeping with the early transcriptomic, genomic and epigenetic changes already present
137 in MBL as well as the known increased risk of infections even at the earliest stages of the
138 disease²². Among the features that distinguished immune and leukemia cells interactions in

139 patients with CLL were an increased number of cellular interactions compared to HDs,
140 especially within myeloid cells, that predominantly involved multiple inhibitory immune signals,
141 and which were no longer detected after ibrutinib treatment. Thus, although T cell deficits in
142 CLL have been well investigated^{23,24}, the contribution of myeloid cells to inhibitory signals has
143 been far less characterized and warrants further assessment.

144

145 **ACKNOWLEDGEMENTS**

146 We thank Jerome Ritz and the DFCI Pasquarello Tissue Bank in Hematologic Malignancies for
147 prospective collection and processing of blood samples from healthy donors. This work was
148 supported in part by the NCI (5P01CA081534-14, P01CA206978, R01CA216273,
149 UG1CA233338). C.J.W. acknowledges support from the CLL Global Research Foundation.
150 SHG was supported by a Kay Kendall Leukaemia Fund Fellowship. EMP acknowledges support
151 from Research funding Doris Duke Charitable Foundation (Physician-Scientist Fellowship),
152 Conquer Cancer (The ASCO Foundation) Young Investigator Award, Dana-Farber Flames
153 FLAIR. J.F acknowledges support from the NIGMS under Award Number R35GM142889. PG
154 acknowledges support from Associazione Italiana per la Ricerca sul Cancro – AIRC, Milano,
155 Italy (Special Program on Metastatic Disease – 5 per mille #21198) and ERA NET
156 TRANSCAN-2 Joint Transnational Call for Proposals: JTC 2016 (project #179 NOVEL), project
157 code (MIS) 5041673. S.L. is supported by the NCI Research Specialist Award (R50CA251956).

158

159 **AUTHORSHIP CONTRIBUTIONS**

160 N.P., J.F., S.H.G. and C.J.W. designed and conceived the study; N.P., L.Z.R., T.J.K., S.L.S.,
161 N.E.K., C.L., T.D.S., P.G., and L.S. collected samples and clinical annotations; S.L. generated

162 the single cell RNAseq libraries and processed the raw sequencing data; N.P., Y.E.T., C.K.L.,
163 N.C., E.M.P., D.S.N., J.F., and S.G. analyzed and interpreted data; J.F., S.G. and C.J.W.
164 supervised the project; N.P., Y.T., S.G., and C.J.W. wrote the paper with assistance from all
165 other authors.

166 **Disclosure of conflict of interest:**

167 N.P. is currently an employee of AstraZeneca; CJW holds equity in BioNTech, Inc.; and
168 receives research funding from Pharmacyclics; SHG has received speaker fees from Janssen UK,
169 travel and honoraria from Abbvie, and undertakes research consultancy for Novalgen Limited.
170 P.G. received honoraria from AbbVie, AstraZeneca, ArQule(MSD, BeiGene,
171 Celgene/Juno/BMS, Janssen, Loxo/Lilly, Roche and research funding from AbbVie,
172 AstraZeneca, Janssen, Sunesis. P.V.K serves on the Scientific Advisory Board to Celsius
173 Therapeutics Inc. and Biomage Inc. N.E.K. Advisory Board for: Abbvie, Astra Zeneca, Behring,
174 Cytomx Therapy, Dava Oncology, Janssen, Juno Therapeutics, Oncotracker, Pharmacyclics and
175 Targeted Oncology. DSMC (Data Safety Monitoring Committee) for: Agios Pharm,
176 AstraZeneca, BMS –Celgene, Cytomx Therapeutics, Janssen, Morpho-sys, Rigel. Research
177 funding from: Abbvie, Acerta Pharma, Bristol Meyer Squib, Celgene, Genentech, MEI Pharma,
178 Pharmacyclics, Sunesis, TG Therapeutics, Tolero Pharmaceuticals. L.S. received honoraria from
179 AbbVie, AstraZeneca, Janssen and travel funding from Janssen. T.D.S. received research support
180 to institution from Genentech, Phamacyclics.

181

182 **REFERENCES**

183 1 Burger J. A. The CLL cell microenvironment. *Adv Exp Med Biol.* 2013;**792**, 25-45.

184 2 Dagklis A., Fazi, C., Scarfo, L., Apollonio, B. & Ghia, P. Monoclonal B lymphocytosis
185 in the general population. *Leuk Lymphoma*. 2009;**50**, 490-492.

186 3 Rawstron A. C., Bennett F.L., O'Connor S.J.M. *et al.* Monoclonal B-cell lymphocytosis
187 and chronic lymphocytic leukemia. *N Engl J Med*. 2008;**359**, 575-583.

188 4 Puente X. S., Beà S., Valdés-Mas R., *et al.* Non-coding recurrent mutations in chronic
189 lymphocytic leukaemia. *Nature*. 2015; **526**, 519-524.

190 5 Agathangelidis, A., Ljungström V., Scarfò L., *et al.* Highly similar genomic landscapes in
191 monoclonal B-cell lymphocytosis and ultra-stable chronic lymphocytic leukemia with low
192 frequency of driver mutations. *Haematologica*. 2018;**103**, 865-873.

193 6 Kretzmer H., Biran A., Purroy N., *et al.* Preneoplastic Alterations Define CLL DNA
194 Methylome and Persist through Disease Progression and Therapy. *Blood Cancer Discov*.
195 2021;**2**(1):54-69.

196 7 Purroy N., Wu CJ. Coevolution of leukemia and host immune cells in Chronic
197 Lymphocytic Leukemia. *Cold Spring Harb Perspect Med*. 2017;**7**(4):a026740.

198 8 Plass M., Solana J., Wolf F.A., *et al.* Cell type atlas and lineage tree of a whole complex
199 animal by single-cell transcriptomics. *Science*, 2018; 360(6391):eaaq1723.

200 9 Villani A. C., Satija R., Reynolds G., *et al.* Single-cell RNA-seq reveals new types of
201 human blood dendritic cells, monocytes, and progenitors. *Science*, 2017;**356**(6335):eaah4573.

202 10 Navin,N., Kendall J., Troge J., *et al.* Tumour evolution inferred by single-cell sequencing.
203 *Nature*.2011;**472**(7341):90-94.

204 11 Patel A. P., Tirosh I., Trombetta J.J., *et al.* Single-cell RNA-seq highlights intratumoral
205 heterogeneity in primary glioblastoma. *Science*. 2014;**344**(6190):1396-1401.

206 12 Tirosh I., Izar B., Prakadan S.M., *et al.* Dissecting the multicellular ecosystem of
207 metastatic melanoma by single-cell RNA-seq. *Science*. 2016;352(6282):189-196.

208 13 Gohil S.H., Iorgulescu J.B., Braun D.A., Keskin D.B., Livak K.J. Applying high-
209 dimensional single-cell technologies to the analysis of cancer immunotherapy. *Nat Rev Clin*
210 *Oncol*. 2021 Apr;18(4):244-256.

211 14 Roerink S. F., Sasaki N., Lee-Six H., *et al.* Intra-tumour diversification in colorectal
212 cancer at the single-cell level. *Nature*. 2018;556(7702):457-462.

213 15 Gruber M., Bozic I., Leshchiner I., *et al.* Growth dynamics in naturally progressing
214 chronic lymphocytic leukemia. *Nature*. 2019;570(7762):474-479.

215 16 Zheng G. X., Terry J.M., Belgrader P., *et al.* Massively parallel digital transcriptional
216 profiling of single cells. *Nat Commun*. 2017; **8**:14049.

217 17 Hao Y., Hao S., Andersen-Nissen E., *et al.* Integrated analysis of multimodal single-cell
218 data. *Cell*. 2021;184(13):3573-3587.e29.

219 18 Massoni-Badosa R., Iacono G., Coutinho C. *et al.* Sampling time-dependent artifacts in
220 single-cell genomics studies. *Genome Biol*. 2020;21(1):112

221 19 Efremova M., Vento-Tormo M., Teichmann S.A., Vento-Tormo R. CellPhoneDB:
222 inferring cell–cell communication from combined expression of multi-subunit ligand–receptor
223 complexes. *Nat Protoc*. 2020;15(4), 1484-1506.

224 20 Rendeiro A.F., Krausgruber T., Fortelny N., *et al.* Chromatin mapping and single-cell
225 immune profiling define the temporal dynamics of ibrutinib in CLL. *Nat Commun*.
226 2020;11(1):577.

227 21 Gutierrez C., Al'Khafaji A.M., Brenner E., et al. Multifunctional barcoding with
228 ClonMapper enables high-resolution study of clonal dynamics during tumor evolution and
229 treatment. *Nature Cancer*. 2021; **2**:758–772.

230 22 Moreira J., Rabe K.G., Cerhan J.R., et al. Infectious complications among individuals
231 with clinical monoclonal B-cell lymphocytosis (MBL): a cohort study of newly diagnosed cases
232 compared to controls. *Leukemia*. 2013;27(1):136-41.

233 23 Ramsay A.G., Johnson A.J., Lee A.M., et al. Chronic lymphocytic leukemia T cells show
234 impaired immunological synapse formation that can be reversed with an immunomodulating
235 drug. *J Clin Invest*. 2008;118(7):2427-37.

236 24 Long M., Beckwith K., Do P., et al. Ibrutinib treatment improves T cell number and
237 function in CLL patients. *J Clin Invest*. 2017;127(8):3052-3064.

238

239 **FIGURE LEGENDS**

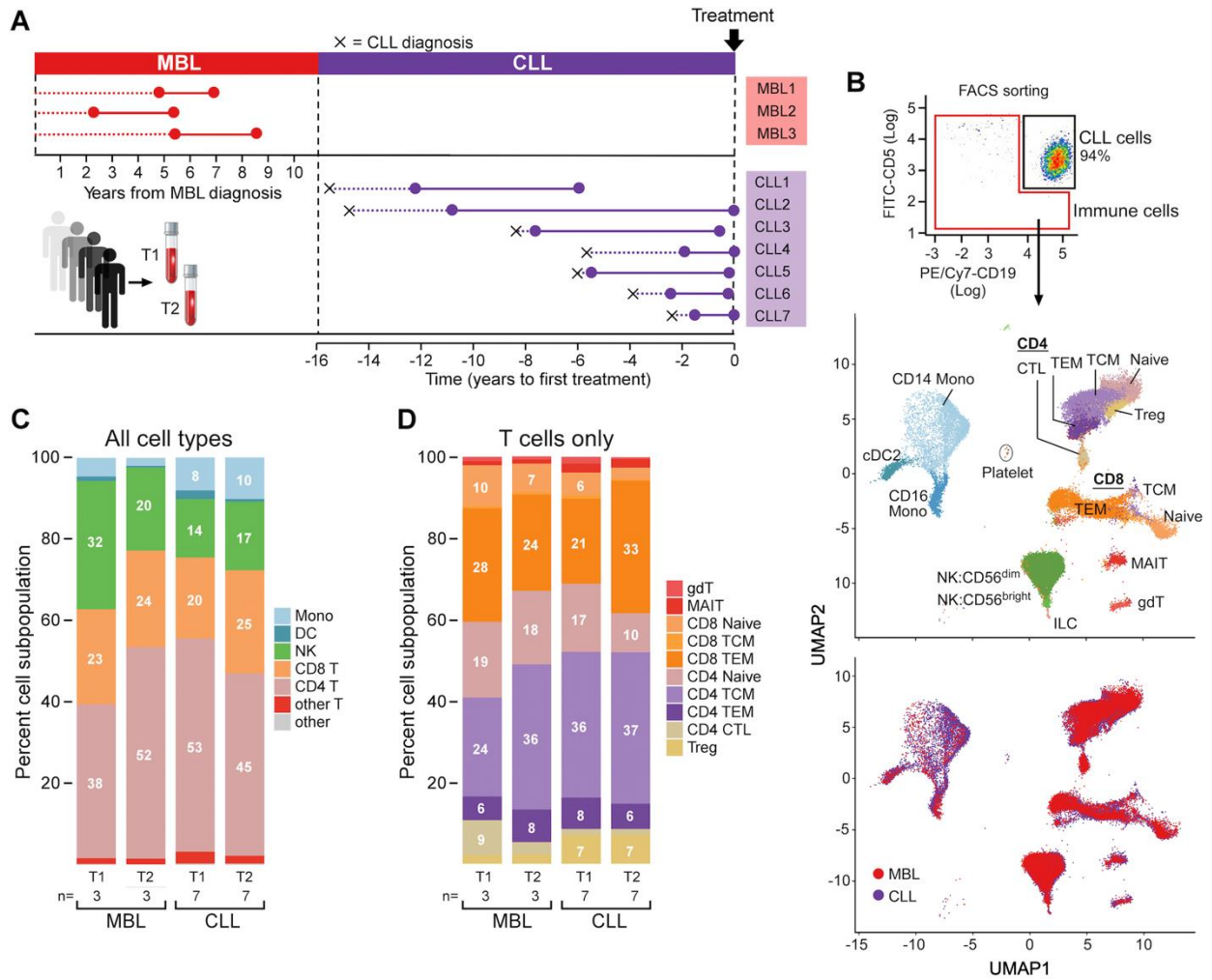
240 **Figure 1. scRNAseq analysis of immune cells from non-progressive MBL patients and CLL**
241 **patients. (A)** Peripheral blood mononuclear cells from 2 serial samples were collected for 3
242 MBL (red dots) and 7 CLL patients (purple dots). **(B)** Non-CD19⁺CD5⁺ cells were isolated by
243 fluorescence-activated cell sorting. Uniform manifold approximation and projection (UMAP)
244 visualization of all immune cells. Cells are colored by immune cell type (top) and CLL or MBL
245 assignment (bottom). **(C)** Proportion of immune cell types per time point in MBL and CLL
246 patients. **(D)** Proportion of T cell types per time point in MBL and CLL patients. Cell
247 percentages were calculated after averaging cell numbers from all samples. Abbreviations: DC,
248 Dendritic cell; pDC, Plasmacytoid dendritic cell; Mono, Monocyte; T, T-cell; NK, Natural killer
249 cell; ILC, Innate lymphoid cells; gdT, Gamma-delta T cells; MAIT, Mucosal associated invariant
250 T cells; TCM, Central memory T cells; TEM, Effector memory T cells; CTL, Cytotoxic T cells;
251 Treg, Regulatory T cells.

252 **Figure 2. scRNAseq analysis of immune cells from healthy donors and progressive disease**
253 **from MBL to CLL. (A)** scRNAseq was performed on PBMCs collected from 4 MBL patients
254 (red dots) that progressed to CLL (purple dots), and from 2 healthy donors (blue dots). Symbol X
255 indicates the time of diagnosis of CLL. **(B)** UMAP visualization of all immune cells colored by
256 immune cell types (left) and by sample types (right). **(C)** Proportion of immune cell types (left)
257 and T cell subtypes (right). **(D)** Number of significant differentially expressed genes for each cell
258 type by performing comparison of paired samples within patients (left panel) or comparison
259 between MBL samples or CLL samples versus healthy donors (right panel). Cells were

260 categorized based on lymphoid and myeloid cells. (E) Same analysis for significant differentially
261 expressed genes was performed on 3 independent non-progressive MBL patients and 7 CLL
262 patients (from **Figure 1**). (F) Heatmaps with the number of the significant ligand-receptor
263 interactions for each cell type under different conditions using CellPhoneDB v2.1.7. Heatmap
264 comparing the number of significant interactions between healthy donors and patient samples
265 from either MBL stage or CLL stage (left). Heatmaps including samples before and after
266 ibrutinib for two additional patients (right panels). Grey boxes indicate insufficient number of
267 cells to perform interactome analysis. (G) Heatmaps representing the difference of p-values for
268 each ligand-receptor pair regarding specific cell types (x-axis). Interactions that are enriched in
269 patients (red) or enriched in healthy donors (blue) were calculated by subtracting $-\log_{10}(\text{p-value})$ in
270 healthy donors from $-\log_{10}(\text{p-value})$ in patients (left panel). The same interactions that are either
271 enriched (red) or depleted (blue) after ibrutinib (right panels) are calculated by subtracting $-\log_{10}(\text{p-value})$ in pre-ibrutinib from $-\log_{10}(\text{p-value})$ in post-ibrutinib. Abbreviations: HDs, Healthy
273 donors; Pts, Patients; cell type abbreviations are the same as in **Figure 1**.
274

275
276
277
278

Figure 1



279

280

281

282

283

284

285

286

287

288 **Figure 2**

